Food Chemistry 459 (2024) 140334

Contents lists available at ScienceDirect

Food Chemistry

journal homepage: www.elsevier.com/locate/foodchem

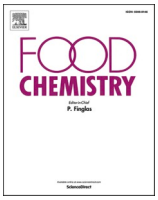

Uncovering phytochemicals quantitative evolution in avocado fruit mesocarp during ripening: A targeted LC-MS metabolic exploration of *Hass*, *Fuerte* and *Bacon* varieties

Irene Serrano-García [a], Carlos Saavedra Morillas [a], María Gemma Beiro-Valenzuela [a], Romina Monasterio [a,b], Elena Hurtado-Fernández [c], José Jorge González-Fernández [d], José Ignacio Hormaza [d], Romina Pedreschi [e,f], Lucía Olmo-García [a,*], Alegría Carrasco-Pancorbo [a]

[a] Department of Analytical Chemistry, Faculty of Sciences, University of Granada, Ave. Fuentenueva s/n, 18071 Granada, Spain
[b] Instituto de Biología Agrícola de Mendoza (IBAM), UNCuyo - CONICET, Facultad de Ciencias Agrarias, Chacras de Coria, Mendoza 5505, Argentina
[c] Department of Biological and Health Sciences, Faculty of Health Sciences, University of Loyola, Campus Sevilla, Avda. de las Universidades S/N, 41704 Dos Hermanas, Spain
[d] Institute for Mediterranean and Subtropical Horticulture (IHSM La Mayora-UMA-CSIC), 29750, Algarrobo-Costa, Málaga, Spain
[e] Escuela de Agronomía, Facultad de Ciencias Agronómicas y de los Alimentos, Pontificia Universidad Católica de Valparaíso, Calle San Francisco S/N, La Palma, Quillota 2260000, Chile
[f] Millennium Institute Center for Genome Regulation (CRG), Santiago 8331150, Chile

ARTICLE INFO

Keywords:
Persea americana Mill.
Phenolic compounds
Amino acids
Nucleosides
Vitamins
Phytohormones

ABSTRACT

Avocado ripening entails intricate physicochemical transformations resulting in desirable characteristics for consumption; however, its impact on specific metabolites and its cultivar dependence remains largely unexplored. This study employed LC-MS to quantitatively monitor 30 avocado pulp metabolites, including phenolic compounds, amino acids, nucleosides, vitamins, phytohormones, and related compounds, from unripe to overripe stages, in three commercial varieties (*Hass*, *Fuerte*, and *Bacon*). Multivariate statistical analysis revealed significant metabolic variations between cultivars, leading to the identification of potential varietal markers. Most monitored metabolites exhibited dynamic quantitative changes. Although phenolic compounds generally increased during ripening, exceptions such as epicatechin and chlorogenic acid were noted. Amino acids and derivatives displayed a highly cultivar-dependent evolution, with *Fuerte* demonstrating the highest concentrations and most pronounced fluctuations. In contrast to penstemide, uridine and abscisic acid levels consistently increased during ripening. Several compounds characteristic of the *Bacon* variety were delineated but require further research for identification and role elucidation.

1. Introduction

The avocado (*Persea americana* Mill.) holds significant socio-economic importance and is highly valued both as fresh fruit and a versatile ingredient in various recipes. *P. americana* is a polymorphic species comprising several subspecies or horticultural races capable of hybridizing and producing a wide array of cultivars differing in botanical traits and edaphoclimatic preferences (Talavera et al., 2023). The global avocado industry is overwhelmingly dominated by *Hass*, accounting for 95% of commercial production due to its excellent pulp quality, higher yield, good and late on-tree storage, extended shelf-life, high oil content and resistance to transport (Crane et al., 2013; Pedreschi et al., 2019). Other commercial hybrids include *Fuerte* and *Bacon* varieties, which are significant in Spain, the leading avocado producer in Europe (FAO, 2023). Spain grows approximately 80% of *Hass*, 12% of *Fuerte*, 5% of *Bacon*, and 3% of other varieties (Cascallar, 2020).

Avocado fruit development comprises diverse physiological stages from cell division and enlargement during growth to lipid accumulation during maturation (Kassim et al., 2013). Unlike many other fruits, avocado maturation is primarily marked by the accumulation of lipids rather than carbohydrates and organic acids (Pedreschi et al., 2019). Both phases contribute to reach the fruit's physiological maturity, which

* Corresponding author.
E-mail address: luciaolmo@ugr.es (L. Olmo-García).

https://doi.org/10.1016/j.foodchem.2024.140334
Received 11 March 2024; Received in revised form 14 June 2024; Accepted 2 July 2024
Available online 4 July 2024

is an essential indicator for determining the optimal harvesting time. The degree of maturity at harvest significantly impacts fruit quality and post-harvest ripening uniformity, thereby influencing consumer acceptance (Núñez-Lillo et al., 2023). Avocado ripening occurs exclusively several days after harvest, marked by complex physiological and biochemical changes involving compound synthesis and degradation. As a climacteric fruit, avocado ripening is associated with an autocatalytic production of ethylene and an increase in the rate of respiration, followed by a decrease as tissue senescence progresses to a state of over ripeness. Three distinct stages in respiration characterize the ripening process: pre-climacteric (minimum respiration), climacteric (peak respiration) and post-climacteric (decline in respiration) (Hurtado-Fernandez et al., 2016). The most substantial changes occur during the pre-climacteric and climacteric stages, influencing fruit acceptability attributes such as texture, firmness, colour, flavour, and aroma. However, during the post-climacteric stage, fruit quality declines, rendering it more susceptible to pathogen attacks (Kassim et al., 2013), partly attributed to the softening that takes place along ripening due to the activity of cell wall-degrading enzymes (Defilippi et al., 2018).

While fatty acids do not seem to act as respiratory substrates in avocado, C_7 sugars, such as *D*-mannoheptulose and its polyol form perseitol, specific of avocado fruit in contrast to the more common C_6 sugars, play an energetic role (Beiro-Valenzuela et al., 2023; Blakey et al., 2012; Tesfay et al., 2012). These C_7 sugars have also been suggested to inhibit the ripening process while the fruit is still on the tree, as well as to contribute to the antioxidant capacity of the fruit (Cowan, 2004; Tesfay et al., 2010). Even though considerable research efforts have been dedicated to unravelling the physiological patterns of the aforementioned primary metabolites, the exploration of other minor yet equally crucial compounds has been somewhat neglected. For instance, there remains a dearth of knowledge regarding the impact of ripening on amino acid content, despite its significant influence on fruit flavour and quality (Pedreschi et al., 2019). A recent work has partially addressed this question, although it was not the main focus of the study (Pedreschi et al., 2022). Over the last decades, phenolic compounds have gained considerable scientific attention due to their health-promoting biological activity as well as their contribution to various aspects of fruit quality such as colour, flavour, bitterness, astringency, and oxidative stability (Gómez-Maqueo et al., 2020; Tomás-Barberán & Espín, 2001). While extensive information has been generated on the factors influencing phenolic content in avocado mesocarp, including genetic factors, geographical origin, harvesting time or growing conditions, studies specifically focusing on the relationship between ripening and phenolic compounds are limited, as illustrated in Table 1. Most of these studies are relevant contributions but have often been restricted to a limited set of samples (typically covering only two ripening stages) or have not specifically aimed to unravel the complexities of climacteric ripening; instead, they assess the impact of post-harvest management on the concentrations of specific compounds in both green and ripe avocados. Villa-Rodríguez et al. (2011) considered 4 ripening stages but only reported total phenolic contents. These same authors have recently carried out more detailed work analysing the dynamics of specific individual metabolites such as phenolic compounds, carotenoids, tocopherols, etc. at four different ripening stages (Villa-Rodriguez et al., 2020). However, such research is still restricted to a limited number of metabolites. In addition, most authors have focused on the *Hass* variety, largely overlooking possible cultivar-dependent factors.

The evident information gap highlighted above underscores the imperative for more comprehensive investigations. Consequently, employing liquid chromatography coupled with mass spectrometry (LC-MS), a total of 30 distinct metabolites including amino acids, nucleosides, vitamins, phytohormones, phenolic compounds, and related substances were meticulously identified and quantified in *Hass*, *Fuerte*, and *Bacon* avocado varieties at four ripening stages, ranging from green to slightly overripe fruits. The primary objectives of this study are as follows: (i) to assess the influence of ripening on the metabolic profile and the most notable compounds affected by this physiological process, (ii) to delineate the individual trends of the various metabolites across the diverse ripening stages, elucidating how their concentrations change over time, and (iii) to investigate whether the avocado variety directly influences metabolic evolution, examining if there are varietal differences in metabolite composition and ripening dynamics.

2. Materials and methods

2.1. Chemical and reagents

LC-MS grade methanol (MeOH) and acetronitrile (ACN) were supplied by VWR Chemicals BDH® (Radnor, PA, EE.UU.). Ultra-pure water with a conductivity of 18.2 MΩ was obtained using a Milli-Q purification system from Millipore (Bedford, MA, USA). Acetic acid (AcH), used to acidify the mobile phase, was purchased from Sigma-Aldrich (St. Louis, MO, USA), as well as the pure standards of uridine (CAS 58-96-8), abscisic acid (CAS 14375-45-2), phenylalanine (CAS 150-30-1), pantothenic acid (CAS 137-08-6), tryptophan (CAS 54-12-6), ferulic acid (CAS 537-98-4), chlorogenic acid (CAS 327-97-9), epicatechin (CAS 490-46-0) and *p*-coumaric acid (CAS 501-98-4). Avocado extracts and pure standard solutions were filtered through a Acrodisc™ 0.22 μm syringe filters with nylon membrane, while mobile phases were filtered through Nylaflo™ 0.45 μm nylon membrane filter, both from Pall Corporation (Michigan, USA).

2.2. Plant material and avocado pre-treatment

Avocados fruits cv. *Bacon*, *Fuerte* and *Hass* were provided by The Institute for Mediterranean and Subtropical Horticulture "La Mayora" (IHSM La Mayora-CSIC-UMA). A total of 100 green fruits per variety were harvested at the end October for cv. *Bacon*, early November for cv. *Fuerte* and mid-March for cv. *Hass* during 2021–2022 season from the orchards of IHSM La Mayora-CSIC-UMA located in Algarrobo-Costa, Málaga (Spain). The choice of harvest time was based on ensuring similarity of dry matter (DM) content, which was measured according to the AOAC 920.151 method once the fruit was removed from the tree (AOAC, 2016). Unripe *Bacon* fruits displayed DM values around 27 ± 2, while *Fuerte* and *Hass* avocados had DM values of 29 ± 3 and 28 ± 2, respectively. After the DM measurement, a total of 80 avocados per variety were selected and grouped into batches of 20 for the controlled ripening process. Unripe avocados (RS1, strongly firm) were processed immediately upon arrival in the laboratory in groups of four, to obtain five biological replicates of each stage ($n = 5$, each consisting of 4 fruits). The remaining avocados were kept in a well-ventilated place at 20–25 °C to simulate domestic handling for a total of two weeks. Avocados at the intermediate stage of ripening (RS2, firm but slightly softening) underwent processing 4–5 days after harvest, while processing of ripe (RS3, ready-to-eat stage) and overripe (RS4, overly soft texture) fruits started at 8–9 and 12–14 days, respectively. The handling of each biological replicate involved the following process: peeling, cutting, bagging, freezing, freeze-drying and grinding to homogenise the particle size. In total, 60 avocado samples (20 samples for each variety, comprising 5 samples × 4 ripeness stages) were obtained and stored at −23 °C until use.

2.3. Sample preparation and LC-MS analysis

A solid-liquid extraction protocol was used to extract the metabolites present in the avocado pulp matrix. A 0.25 g fraction of freeze-dried avocado powder was mixed with 20 mL of a MeOH:H_2O (80:20, v/v) solution in a Falcon tube using a vortex. The mixture was then placed in an ultrasound-assisted bath for 30 min to ensure complete metabolite extraction. Subsequently, the Falcon tube was centrifuged for 5 min at 9000 rpm to separate the liquid phase from the remaining solid, and a second extraction cycle was performed following the same procedure. After pooling both supernatants, they were evaporated under vacuum

Table 1
Studies assessing ripening dynamics in avocados listing the analytical methodologies used and the determinations made in each study. Papers are ordered by their published date.

Cultivar	Ripening Stages	Sample Info	Methodology	Analytical Determinations	Observations	Reference
Hass	Transport from orchard within 3 days (5–7 °C) RS1 (0 days after reception) RS2 (4 days) RS3 (8 days) RS4 (12 days)	60-fruit batch, a sub-batch of 25 avocados per RS (ripening at 15 °C)	GC–MS GC-TCD-FID UV-VIS	Respiration rate and ethylene production Physicochemical parameters Fatty acids content Total phenolic and flavonoid content Antioxidant capacity assays	First comprehensive study of climacteric ripening dynamics with several determinations and RS.	(Villa-Rodríguez et al., 2011)
13 avocado varieties*	Unripe (at harvest time) Ripe (ready-to-eat stage)	Pulp of 3–4 pieces of fruit to compose a sample for each RS and variety	UHPLC-UV/ESI-TOF MS	Twenty metabolites including phenolic acids and related compounds, quinic acid, succinic acid, pantothenic acid, abscisic acid, and flavonoids	First comprehensive characterisation of C_{18} avocado pulp profile Multivariate statistical analysis to discriminate varieties and RS	(Hurtado-Fernández et al., 2011)
Booth 7	Unripe (1 day after harvest) 2 day-intervals for firmness Daily for ethylene production 3-d intervals for the rest of analysis	≈ 135 fruits	GC-PDHID	Fruit firmness and ethylene production Total phenolics and flavonoids assay Total antioxidant capacity Enzyme assays	The study primarily focused on investigating changes in preclimacteric stage avocado fruit treated with aqueous 1-methylcyclopropene and then ripened at 20 °C	(Zhang et al., 2013)
13 avocado varieties*	Unripe (at harvest time) Ripe (ready-to-eat stage)	Pulp of 3–4 pieces of fruit to compose a sample for each RS and variety	GC-FID/APCI-TOF MS	Analysis of 27 metabolites belonging to different chemical families	Evaluation of the potential of GC-APCI-MS in Food Metabolomics and comparison with GC-FID Multivariate statistical analysis to discriminate varieties and RS	(Hurtado-Fernández et al., 2014)
13 avocado varieties*	Unripe (at harvest time) Ripe (ready-to-eat stage)	Pulp of 3–4 pieces of fruit to compose a sample for each RS and variety	GC-APCI-TOF MS	Non-targeted metabolic profiling	Multivariate statistical analysis to discriminate varieties and RS	(Hurtado-Fernández et al., 2015)
Hass	Edible ripeness Over ripeness	≈ 10 kg of fruits	HPLC-DAD-ESI-QTOF-MS HPLC-FLD-MS	Phenolic and other polar compounds Flavan-3-ols	The main objective of this study was to evaluate the distribution of specific metabolites across the seed, peel, and pulp	(López-Cobo et al., 2016)
Bacon, Fuerte, Hass, Orotawa, Pinkerton, Rincon	Unripe (at harvest time) Ripe (ready-to-eat stage)	Not specified	UHPLC-HESI-Q Orbitrap MS	Phenolic compounds (18) Total phenolics	Many compounds were not detected on the samples. Concentration of gentisic and *p*-coumaric acid increased over ripening	(Di Stefano et al., 2017)
Hass	Transport from orchard within 3 days (5–7 °C) RS1 (0 days after reception) RS2 (4 days) RS3 (8 days) RS4 (12 days)	60-fruit batch, a sub-batch of 15 avocados per RS (ripening at 15 °C)	HPLC-DAD HPLC-FLD GC-FID	Individual phenolic compounds (7), carotenoids (6), tocopherols (3), phytosterols (3) Cytotoxic activity	Study and discussion of several individual metabolites throughout the climacteric period.	(Villa-Rodriguez et al., 2020)
Hass	Unripe (0 days) Cold storage: 22 days and 37 days Edible ripeness: fruits after 22- and 37-days of storage	Ten independent fruits per sampling point	GC-TQ MS GC-FID HPLC-FLD UV-VIS UPLC-QTOF-PDA	Sugars and organic acids Fatty acids content and profile Tocopherols content Phytosterol content Total phenolics and antioxidant capacity Individual phenolic compounds	The primary objective of this study was to conduct a thorough phytochemical characterisation of *Hass* avocados throughout three harvest seasons, including from harvest, after cold storage and subsequent shelf-life period to reach edible ripeness.	(Campos et al., 2020)
Pinkerton	Unripe (at harvest time) Ripe (ready-to-eat stage)	No specified	HPLC-PDA	Oil content and fatty acid composition Total phenolic and antioxidant activity Determination of phenolic compounds	This study mainly aimed to characterize the oil, bioactive properties and phytochemicals present in the pulp, seed, and peel of unripe and ripe avocado fruit dried using air, microwave or oven.	(Babiker et al., 2021)
Hass	Unripe (at harvest time) Ripe (ready-to-eat stage)	≈ 400 fruits for the whole study	GC–MS UPLC-PDA	Fatty acids Polar metabolites (sugars, amino acids, etc.) Phenolic compounds Abscisic acid In-vitro hydrophilic and lipophilic antioxidant capacity	One of the first study paying attention to the composition of the amino acid and its relationship with softening phenomenon in avocado fruit	(Pedreschi et al., 2022)

* **Avocado varieties info:** *ColinV 33, Gem, Harvest, Hass, Hass Motril, Jiménez 1, Jiménez 2, Lamb Hass, Marvel, Nobel, Pinkerton, Sir Prize, Tacambaro;* **Abbreviations in alphabetical order:** APCI: Atmospheric pressure chemical ionisation; DAD: Diode array detector; ESI: Electrospray ionisation; FID: Flame ionisation detector; FLD: Fluorescence detector; GC: Gas chromatography; HESI: Heated electrospray ionisation source; HPLC: High pressure liquid chromatography; MS: Mass spectrometry; PDA: Photodiode array detector; PDHID: Discharge helium ionisation detector; Q: Quadrupole; RS: Ripening stage; TCD: Thermal conductivity detector; TOF: Time-of-flight; TQ: Triple quadrupole; UHPLC: Ultra-high pressure liquid chromatography; UV-VIS: Ultra violet-visible spectrophotometry.

conditions and resuspended in 1 mL MeOH/H_2O (80:20, v/v). The liquid was filtered and transferred into an amber glass LC-vial.

External calibration curves, used for quantitative purposes, were prepared by diluting the required amount of each commercial standard in the appropriate volume of MeOH:H_2O (80:20, v/v). A quality control (QC) sample, prepared from a solid portion of each avocado sample, was used to check the instrumental status over the sequences. All standard solutions and avocado extracts were stored at −23 °C until used.

Two distinct LC-MS platforms were used for sample analysis. An Elute series Ultra High Performance Liquid Chromatography (UHPLC) equipped with an electrospray source (ESI) and coupled to the compact QTOF high-resolution spectrometer from Bruker Datonics (Bremen, Germany) conducted the qualitative avocado characterisation based on its mass accuracy and its ability to perform MS/MS experiments. In addition, an InfinityAgilent 1260 series modular liquid chromatography system (Agilent Technologies, Waldbronn, Germany) coupled to a Bruker Esquire 2000 series Ion Trap (IT) mass spectrometer (LC-ESI-IT MS) by means of an ESI source was used for quantitative purposes. Both instruments were equipped with a Zorbax Eclipse Plus C_{18} column (4.6 × 150 mm, 1.8 μm particle size) from Agilent Technologies. Chromatographic conditions were reproduced from the report of Serrano-García et al. (2023). To achieve the separation of the metabolites was necessary to use a mobile phase A consisting of Milli-Q ultra-pure water (0.5% acetic acid) and acetonitrile as mobile phase B, with a flow rate of 0.8 mL/min. A gradient elution was applied: 0 min, 95% A; 22 min, 25% A; 23 min, 0% A, 23.5 min; 0% A; and at 25 min return to initial conditions. Injection volume was 10 μL. ESI operated in negative polarity and *Full Scan* mode (within the range *m/z* 50–1000). Source parameters were adapted to the MS systems conditions as follows: 30 psi of nebuliser pressure, 9 L min^{-1} and 300 °C of drying gas flow and temperature, respectively, and + 3200 V capillary voltage on the IT MS system. In the QTOF MS system, the selected conditions were as follows: 3.0 Bar of nebuliser pressure, 9 L min^{-1} and 220 °C of drying gas and + 4500 V capillary voltage. Auto MS/MS fragmentation was carried out to facilitate compound identification. A predetermined absolute threshold of 1000 counts was chosen for precursor ion collection, alongside a cycle time of 1 s. Collision energy stepping factors varied within the range of 0.2% to 0.8%. The software controlling LC-IT MS comprised Agilent ChemStation and Bruker Esquire control, whilst LC-QTOF MS used Compass Hystar and Otof Control. Data treatment was done with Data Analysis 4.0 from Bruker Daltonics.

2.4. Analytical parameters of the method

Pure standard solutions and QC samples were used to evaluate the main analytical parameters of the method such as the linearity, limits of detection (LOD) and quantification (LOQ) and repeatability *intra-* and *inter-* day. The external calibration curves were obtained by linear regression using the least squares method. Each point of the curves corresponded to the mean of three independent injections. Metabolites were quantified using the corresponding pure standard or, if not available, with a compound of the same chemical category. Thus, glycosylated and derived forms of coumaric acid were quantified with the *p*-coumaric acid standard. Also, the hexoses of dihydroxybenzoic acid, the glucoside of caffeic acid and unknown metabolites. The ferulic acid pure standard was used to quantify its glycosylated form. Phenylalanine calibration curves were used to quantify tyrosine, *N*-acetyl-tyrosine and *N*-acetyl-phenylalanine. Finally, using the tryptophan pure standard, the *N*-acetyl-tryptophan content was assessed. The other metabolites were quantified using their corresponding pure standard.

LOD and LOQ values were estimated using the lowest injected concentration of each standard and calculating the concentration generated with a signal-to-noise ratio (S/N) equal to 3 and 10, respectively. *Intra-*day and *inter-*day repeatability, expressed as coefficient of variation (% CV), were obtained from data of quality control injections performed on the same day or on different days.

2.5. Statistical analysis

Quantitative data were expressed as mean ± standard deviation (SD) ($n = 5$) and analysed using InfoStat 2020 software. Due to the non-normal distribution of the data, a non-parametric Kruskal-Wallis test was first performed. This was followed by pairwise comparisons using the Mann-Whitney test. Statistical significance was established with *p*-values less than $\alpha = 0.05$. SIMCA v14.1 software was used for the execution of an unsupervised principal component analysis (PCA) with a data matrix consisting of 60 samples (observations) and 30 variables (metabolites) expressed as concentration (mg kg^{-1} DW). The heat map was performed in MetaboAnalyst 5.0 software with the Euclidean distance measure and the ward clustering algorithm. Autoscaling was applied as a preprocessing step for compound normalisation.

3. Results and discussion

3.1. Targeted metabolite characterisation

A targeted characterisation of the sample extracts was performed using LC-ESI-QTOF MS/MS. A total of 30 compounds were selected from the metabolic profile based on their predominance in the profile and/or potential relationship with the avocado ripening progression. Metabolite identification was based on the interpretation of the accurate mass information, predicted molecular formula (error ≤ 5 ppm), relative elution order and fragmentation patterns, which were compared with previous relevant reports (Campos et al., 2020; Hurtado-Fernández et al., 2011; López-Cobo et al., 2016; Serrano-García et al., 2023), public MS/MS databases (*MassBank*, *MoNA*, *FoodDB*,..) and *in-silico* fragmentation MetFrag tool (Ruttkies et al., 2016). Table 2 lists the selected metabolites, which include a wide range of metabolite groups, such as nucleosides, amino acids and related compounds, phenolic compounds, vitamins, phytohormones and iridoids. It should be noted that while several compounds could not be reliably annotated, they were included in any case due to their relevance within the metabolic profile.

3.1.1. Amino acids, nucleosides, and related compounds

Seven metabolites were tentatively classified within the group of nucleosides, amino acids, and *N*-acetyl-amino acid derivatives. Briefly, the chromatographic peaks at 2.7, 2.9, 4.9 and 6.4 min were identified as uridine (exhibiting a predominant signal at *m/z* 243.0622 $[M-H]^-$), tyrosine (*m/z* 180.0665 $[M-H]^-$), phenylalanine (*m/z* 164.0718 $[M-H]^-$) and tryptophan (*m/z* 203.0826 $[M-H]^-$), respectively, based on the comparison with their pure standards. The peak appearing at 6.7 min with an MS signal at *m/z* 222.0770 $[M-H]^-$ and main fragments at *m/z* 180, 163, 119, 107 and 58 was tentatively assigned as *N*-acetyl-tyrosine, according to the predicted molecular formula provided considering the accurate mass and the fragmentation pattern. Similarly, the peak eluting at 9.6 min and mass spectrum dominated by the signal *m/z* 206.0824 $[M-H]^-$ was tentatively assigned to *N*-acetyl-phenylalanine. Lastly, the peak with a retention time of 10.3 min and molecular formula $C_{13}H_{14}N_2O_3$ was consistent with *N*-acetyl-tryptophan, according to ion descriptors, relative elution order and fragmentation pattern. This latter compound is being described for the first time in avocado.

3.1.2. Phenolic compounds and derivatives

Fifteen phenolic compounds constituted the largest chemical group of metabolites quantified in avocado pulp. The different annotated compounds will be described in order of appearance in the chromatographic profiles.

The peaks at 4.2 and 4.5 min, with the molecular formula $C_{13}H_{18}O_8$, were tentatively identified as phenolic glycosides known as isotachioside (4-hydroxy-2-methoxyphenyl-1-*O*-*β*-glucopyranoside) and tachioside (4-hydroxy-3-methoxyphenyl-1-*O*-*β*-D-glucopyranoside), respectively. This identification was based, among other reasons, on the 0.9215 score predicted by MetFrag from MS data and the fragmentation pattern. While

Table 2
Overview of compounds identified (or with a tentative identity assigned) in the avocado samples under study.

Proposed Compound	Chemical Family	Formula	Rt (min)	m/z_{exp}	m/z_{theo}	Δ m/z (ppm)	mSigma	Main MS/MS fragments (% relative abundance)
Uridine	Nucleoside	$C_9H_{12}N_2O_6$	2.7	243.0622	243.0623	0.1	5.1	110.03 (100), 82.03 (43), 122.02 (13), 152.03 (9)
Tyrosine	Amino acid	$C_9H_{11}NO_3$	2.9	180.0665	180.0666	0.7	10.7	119.05 (100), 163.04 (62), 93.03 (23), 106.04 (20)
Unknown 1	–	$C_{14}H_{26}O_{11}$	3.0	369.1402	369.1402	0.2	4.7	59.02 (100), 73.03 (80.7), 101.02(69), 161.05 (57), 237.09 (29)
Isotachoside	Phenolic compound	$C_{13}H_{18}O_8$	4.2	301.0931	301.0929	−0.8	9.2	123.01 (100), 138.03 (20), 124.01 (7), 139.04 (5)
Dihydroxybenzoic acid hexose I	Phenolic compound	$C_{13}H_{16}O_9$	4.2	315.0722	315.0722	−0.2	4.0	108.02 (100), 152.01 (92), 315.07 (55), 109.03 (27), 153.02 (25)
Tachioside	Phenolic compound	$C_{13}H_{18}O_8$	4.5	301.0929	301.0929	0.1	12.0	123.01 (100), 138.03 (35), 124.01 (8), 139.04 (5)
Phenylalanine	Amino acid	$C_9H_{11}NO_2$	4.9	164.0718	164.0717	−0.7	5.1	103.05 (100), 72.01 (60), 147.04 (46)
Dihydroxybenzoic acid hexose II	Phenolic compound	$C_{13}H_{16}O_9$	5.0	315.0723	315.0722	−0.5	4.8	153.02 (100), 109.03 (97), 315.07 (60), 152.01 (29), 108.02 (14)
Unknown 2	–	$C_{13}H_{22}O_{10}$	5.0	337.1138	337.1140	0.6	3.9	193.07 (100), 57.03 (74), 101.02 (54), 161.05 (6)
Pantothenic acid	Vitamin	$C_9H_{17}NO_5$	5.2	218.1036	218.1034	−0.9	8.2	146.08 (100), 71.05 (97), 88.04 (77)
Unknown 3	–	$C_{15}H_{26}O_{11}$	5.6	381.1401	381.1402	0.3	18.2	237.10 (100), 59.01 (71), 57.03 (71), 125.03 (24), 279.11 (12), 161.04 (5)
Tryptophan	Amino acid	$C_{11}H_{12}N_2O_2$	6.4	203.0826	203.0826	−0.1	0.9	116.05 (100), 74.03 (41), 142.07 (24)
Penstemide	Iridoid	$C_{21}H_{32}O_{10}$	6.5	443.1922	443.1923	0.1	3.6	443.19 (100), 59.01 (7), 101.02 (6), 113.02 (4)
Caffeic acid glucoside	Phenolic compound	$C_{15}H_{18}O_9$	6.5	341.0878	341.0878	0.1	6.6	161.02 (100), 133.03 (12), 179.03 (10), 59.01 (4)
N-acetyl-tyrosine	Amino acid derivative	$C_{11}H_{13}NO_4$	6.7	222.0770	222.0772	0.8	2.7	180.07 (100), 58.03 (61), 119.05 (58), 107.05 (52), 163.04 (40)
Chlorogenic acid	Phenolic compound	$C_{16}H_{18}O_9$	7.2	353.0879	353.0878	−0.2	4.3	191.06 (100), 89.02 (8)
Coumaric acid hexose	Phenolic compound	$C_{15}H_{18}O_8$	7.5	325.0932	325.0929	−0.8	8.5	145.03 (100), 163.04 (9), 119.04 (7), 59.01 (6)
Ferulic acid hexose	Phenolic compound	$C_{16}H_{20}O_9$	7.9	355.1032	355.1021	0.7	8.3	175.04 (100), 193.05 (20), 160.02 (17), 355.10 (11), 134.04 (9), 59.01 (8)
Epicatechin	Phenolic compound	$C_{15}H_{14}O_6$	8.3	289.0718	289.0718	0.0	6.8	109.03 (100), 123.05 (92), 245.08 (85), 203.07 (77)
Unknown 4	–	$C_{20}H_{28}O_{11}$	8.4	443.1558	443.1554	−1.0	1.9	299.11 (100), 281.10 (78), 57.03 (72), 341.12 (51)
Coumaric acid malonyl-hexose I	Phenolic compound	$C_{18}H_{20}O_{11}$	8.7	411.0931	411.0933	0.3	11.2	145.03 (100), 163.04 (10), 367.10 (8)
Unknown 5	–	$C_{17}H_{28}O_{10}$	8.8	391.1606	391.1610	0.9	1.6	247.12 (100), 57.04 (91), 101.03 (44), 161.04 (35), 113.02 (25)
Coumaric acid malonyl-hexose II	Phenolic compound	$C_{18}H_{20}O_{11}$	9.0	411.0932	411.0933	0.2	9.8	145.03 (100), 163.04 (41), 367.10 (20)
Coumaric acid malonyl-hexose III	Phenolic compound	$C_{18}H_{20}O_{11}$	9.3	411.0932	411.0933	0.2	6.2	145.03 (100), 163.04 (9), 367.10 (9)
Coumaric acid derivative	Phenolic compound	$C_{21}H_{26}O_{12}$	9.4	469.1350	469.1351	0.3	2.6	145.03(100), 163.04 (63), 323.10 (54), 367.10 (34)
N-acetyl-phenylalanine	Amino acid derivative	$C_{11}H_{13}NO_3$	9.6	206.0824	206.0823	−0.5	5.0	117.04 (100), 91.05 (67), 145.03 (62), 164.08 (61), 58.03 (46), 147.05 (44), 103.05 (40)
p-Coumaric acid	Phenolic compound	$C_9H_8O_3$	9.9	163.0400	163.0401	0.3	5.3	119.05 (100), 93.03 (11)
N-acetyl-tryptophan	Amino acid derivative	$C_{13}H_{14}N_2O_3$	10.3	245.0934	245.0932	−0.9	3.9	74.03 (100), 203.08 (67), 116.05 (60), 98.02 (42), 142.07 (28)
Ferulic Acid	Phenolic compound	$C_{10}H_{10}O_4$	10.4	193.0505	193.0506	0.9	3.4	134.04 (100), 178.03 (9)
Abscisic acid	Phytohormone	$C_{15}H_{20}O_4$	13.0	263.1291	263.1289	−0.8	1.4	153.09 (100), 204.12 (69), 219.14 (46)

The prevalent ion detected in the MS spectra of coumaric acid malonyl-hexose I, II and III was $[M\text{-}H\text{-}44]^-$, corresponding to a m/z signal of 367.
>95% of the compounds displayed a score of 100.0.

these compounds have been previously described in other plant matrices, to the best of our knowledge, this is the first time to be reported in avocado. The mass spectra of the peaks detected at 4.2 and 5.0 min showed a common precursor ion at m/z 315.072 $[M-H]^-$, and fragment ions at m/z 108, 109, 152 and 153 (in order from lowest to highest m/z value), which were consistent with isomeric molecules of dihydroxybenzoic acid hexose. The caffeic acid glucoside observed at 6.5 min was identified based on the exact mass and the fragments at m/z 161 and 179, caused from the neutral loss of the glycosidic moiety. The identity of the chromatographic peaks of chlorogenic, *p*-coumaric and ferulic acids was corroborated by comparing retention times and MS spectra with their respective pure standards. Several coumaric acid derivatives and one ferulic acid derivative were detected in the C_{18} metabolic profile of avocado pulp. The peak eluting at 7.5 min was identified as coumaric acid hexose ($C_{15}H_{18}O_8$). The glycosidic form of ferulic acid was detected at m/z 355.1032 (7.9 min). The identity of epicatechin (a flavonoid) at 8.3 min (m/z 289.0718 $[M-H]^-$) was corroborated with its pure standard. In addition, three distinct chromatographic peaks were detected at 8.7, 9.0 and 9.3 min, respectively, which coincided with isomers of coumaric acid malonyl-hexose; the m/z 411 $[M-H]^-$ signal was observed without high intensity in the mass spectrum, while m/z 367 $[M-H\text{-}44]^-$ was the predominant signal. Another coumaric acid derivative was detected at 9.4 min, although the complete structure of the molecule remains partially elucidated.

3.1.3. Other interesting metabolites detected within the profile

The presence of pantothenic acid (also known as vitamin B5) was confirmed at 5.2 min (*pseudo*-molecular ion at *m/z* 218.1036) by comparison with the pure standard. Similarly, abscisic acid (a phytohormone), which appeared in the profile at 13.0 min (*m/z* 263.1291 $[M-H]^-$) was also identified. Following a previously published report, the mass spectrum of the peak with a retention time of 6.5 min at *m/z* 433.1922 $[M-H]^-$ was tentatively noted as penstemide (López-Cobo et al., 2016); it showed slight fragmentation with fragments at *m/z* 113, 101 and 59. Five other compounds with *m/z* 369.1402 ($C_{14}H_{26}O_{11}$), *m/z* 337.1138 ($C_{13}H_{22}O_{10}$), *m/z* 381.1401 ($C_{15}H_{26}O_{11}$), *m/z* 443.1558 ($C_{20}H_{28}O_{11}$) and *m/z* 391.1606 ($C_{17}H_{28}O_{10}$) could not be tentatively identified, but they were included in the analysis because they appeared to exhibit a rather evident evolution throughout ripening. Further experiments are already underway in the lab to gather more information about these compounds.

3.2. Quantitative data

After qualitatively characterising the acquired profiles, we proceeded to define the analytical parameters of the employed methodology. Table 1 of **Supplementary Material** summarises the data extracted for each analytical parameter, including calibration functions, correlation coefficients, quantitative ranges, LODs and LOQs, as well as repeatability. Adequate figures were obtained for R^2 (with values above 0.990 in all cases). The LODs ranged from 5.2 to 35.2 μg L^{-1} and the LOQs from 17.3 to 117.2 μg L^{-1}. *Intra*-day repeatability did not exceed 9.05% and *inter*-day repeatability 10.28%, indicating a correct operating procedure. After checking the methodological reliability, quantification was carried out.

Table 3 summarises the quantitative data obtained through external calibration curves. Despite the absence of pure standards in some cases, preventing absolute quantification, this approach enabled a meaningful comparison of metabolite evolution during climacteric ripening and a thorough assessment against the three evaluated cultivars. Additionally, statistical analyses, essential for drawing significant conclusions, are presented in the same table. Compounds not detected at certain ripening stages were not subjected to pair testing, assuming significance at subsequent stages if the compound was determined in the subsequent level. Consequently, statistically significant differences ($p \leq 0.05$) were not only observed between ripening stages within the same variety but also among the three varieties at corresponding stages. With this initial perspective guiding us, the upcoming sections will delve into untangling these nuances.

3.2.1. Unsupervised exploration of the correlation between the concentrations of the different phytochemicals determined, ripening stages and varieties

The quantitative data set obtained by LC-MS was first examined by applying principal component analysis (PCA). This initial step allowed to assess the overall quality of the data, explore the biological diversity, and identify the main sources of variance and possible natural clustering of the samples. The first two principal components (PC1 and PC2) were considered for the illustration shown in Fig. 1A. For better understanding, the score plot and the loading plot were merged, resulting in the biplot figure. PC1 accounted for 32.2% of the overall variance in the model, followed by PC2 at 26.0%. The inclusion of the third principal component (PC3) contributed an additional 19.5%, resulting in a cumulative variance coverage of 77.7%. This indicates that the first three principal components captured a significant portion of the variability present in the data, allowing for a meaningful interpretation of the results.

The PCA biplot shows clear metabolic differences both with regard to the ripening process of the fruit and the avocado variety examined. The first component (PC1), which explains the largest proportion of the variance, appeared to have a strong influence on the differences in the metabolic profile according to the ripening stage. In general, unripe (RS1) and medium-ripe (RS2) avocados were situated at negative scores of PC1, while ripe (RS3) and overripe (RS4) fruits were situated at positive scores. Notably, early ripening stages RS1 and RS2, especially in *Bacon* and *Fuerte*, displayed closely clustered chemical profiles. However, *Hass* samples RS1 and RS2 exhibited a somewhat less compact grouping. Similarly, the ripe and overripe avocados (RS3 and RS4) manifested overlapping profiles, with *Bacon* and *Hass* presenting the most distinctive metabolic characteristics during the transition from climacteric to post-climacteric stages. The second component (PC2) appeared to facilitate the differentiation of avocado varieties, with *Bacon* situated at positive scores, while *Fuerte* and *Hass* were predominantly situated in the negative zone along its axis.

After verifying the differentiation of the phytochemical profile, possible correlations between cultivar- and ripening-associated metabolites were studied by correlation analysis and interactive visual heat mapping (Fig. 1B). Several key metabolites were preliminarily highlighted as playing a pivotal role in cultivar distinction. Two of the most significant metabolites for varietal discrimination were the two hexose isomers of dihydroxybenzoic acid (characteristic of *Hass* fruits due to their high content). On the other hand, low tachioside concentrations occurred to be typical for the same variety. Two of the compounds that could not be annotated (*m/z* 381 and 391), isotachioside, chlorogenic acid, pantothenic acid and tryptophan, showed remarkably high concentrations in avocado cv. *Bacon* exclusively. Fruits of cv. *Fuerte* stood out for their tyrosine, *N*-acetyl-tyrosine, *N*-acetyl-phenylalanine and *N*-acetyl-tryptophan contents. In relation to metabolic evolution during ripening, several compounds correlated positively with the time elapsed. Among them, the most influential were coumaric acid hexose, *p*-coumaric acid, ferulic acid hexose and ferulic acid. In addition, abscisic acid, unknown 4 (*m/z* 443) and uridine were also correlated. In contrast, penstemide was the most negatively correlated metabolite.

3.2.2. Evolution of metabolites concentration during avocado fruit ripening

In the preceding section, our aim was to delve into the dataset's structure through a general examination using statistical analysis of the quantitative LC-MS data. The subsequent phase involved providing an intricate account of the overarching evolution, categorised by "chemical categories," alongside a detailed portrayal of the individual patterns exhibited by each metabolite throughout all stages of fruit ripening.

As expected, some compounds displayed consistent trends across the three varieties, while others exhibited distinctive behaviour patterns. To enhance clarity and comprehension, this section has been partitioned into two subsections, each complemented by **Figs. 2** and **3**.

3.2.2.1. Delving into phenolic compounds quantitative evolution over time. Plant phenols are generally located in the vacuole and are derived from the shikimate, pentose phosphate and phenylpropanoid pathways (Lin et al., 2016). These secondary metabolites, which include, among others, phenolic acids, flavonoids and lignans, are found in both free and conjugated forms (primarily as *β*-glycosides). Phenolic compounds play many essential roles in plants, influencing sensory attributes such as flavour, taste, and colour, while also playing a crucial role in plant defence mechanisms (Balasundram et al., 2006).

The category of phenolic compounds exhibited a significant ($p \leq 0.05$) response to the ripening process, as demonstrated in the preceding section. Notably, only the isomers of dihydroxybenzoic acid hexose showed no substantial changes. This finding aligns with the observations of López-Cobo et al. (2016), who also found no significant variation in the concentration of one of the isomers of this compound in *Hass* fruit pulp between the optimal time of consumption and the stage of overripening. However, it is worth noting that López-Cobo's study focused solely on these two ripening stages, contrasting with the more comprehensive examination of four ripening stages in our investigation. While these metabolites (isomers of dihydroxybenzoic acid hexose) do

Table 3
Quantitative results of LC-MS analysis of avocado pulp at four different ripening stages for *Hass*, *Fuerte* and *Bacon* varieties.

	Unripe (RS1)			Medium (RS2)			Edible ripeness (RS3)			Overripe (RS4)		
Compound	*Bacon*	*Fuerte*	*Hass*	*Bacon*	*Fuerte*	*Hass*	*Bacon*	*Fuerte*	*Hass*	*Bacon*	*Fuerte*	*Hass*
Amino acids, nucleosides and related compounds												
N-acetyl-phenylalanine	131 ± 42^{abB}	326 ± 77^{abC}	33 ± 8^{aA}	126 ± 34^{abB}	390 ± 32^{bC}	28 ± 10^{aA}	172 ± 32^{bB}	323 ± 67^{aC}	32 ± 8^{aA}	91 ± 17^{aB}	244 ± 56^{aC}	29 ± 1^{aA}
N-acetyl-tryptophan	17 ± 3^{aA}	60 ± 14^{aB}	21 ± 4^{aA}	17 ± 2^{aA}	61 ± 11^{aB}	21 ± 3^{aA}	18 ± 1^{aA}	65 ± 15^{aC}	27 ± 5^{aB}	15 ± 1^{aA}	58 ± 14^{aC}	22 ± 2^{aB}
N-acetyl-tyrosine	17 ± 6^{aA}	52 ± 16^{aB}	21 ± 6^{aA}	23 ± 6^{aA}	135 ± 42^{bB}	27 ± 10^{aA}	59 ± 13^{cA}	250 ± 39^{cC}	114 ± 43^{cB}	43 ± 4^{bA}	259 ± 34^{cB}	59 ± 22^{bA}
Phenylalanine	7 ± 2^{bB}	14 ± 4^{bC}	3.6 ± 0.2^{bA}	22 ± 5^{cB}	30 ± 7^{cC}	2.3 ± 0.7^{abA}	3.2 ± 0.4^{aA}	2.7 ± 0.6^{aA}	2.5 ± 0.4^{aA}	3.2 ± 0.8^{aA}	3 ± 1^{aA}	2.4 ± 0.5^{aA}
Tryptophan	2.8 ± 0.6^{bB}	2.3 ± 0.4^{bB}	1.7 ± 0.2^{bA}	4 ± 1^{cC}	3.1 ± 0.4^{cB}	1.6 ± 0.3^{bA}	5 ± 1^{cB}	1.4 ± 0.3^{aA}	1.2 ± 0.1^{aA}	1.7 ± 0.3^{aA}	1.8 ± 0.5^{abA}	1.4 ± 0.2^{abA}
Tyrosine	6 ± 1^{aA}	15 ± 5^{aB}	4.1 ± 0.2^{aA}	18 ± 5^{bB}	36 ± 10^{bC}	3.2 ± 1^{aA}	6 ± 1^{aB}	110 ± 28^{cC}	3.4 ± 0.8^{aA}	5.6 ± 0.7^{aA}	126 ± 16^{cC}	9 ± 3^{bB}
Uridine	27 ± 9^{aB}	14 ± 3^{aA}	25 ± 5^{aB}	24 ± 9^{aAB}	14 ± 5^{aA}	29 ± 4^{aB}	58 ± 10^{bB}	29 ± 7^{bA}	49 ± 13^{bB}	63 ± 13^{bB}	15 ± 3^{aA}	59 ± 15^{bB}
Iridoid												
Penstemide	38 ± 6^{bB}	51 ± 13^{bB}	27 ± 2^{cA}	34 ± 4^{bB}	43 ± 4^{bC}	18 ± 5^{bA}	23 ± 4^{aB}	17 ± 5^{aAB}	11 ± 3^{aA}	20 ± 2^{aB}	17 ± 2^{aB}	13 ± 3^{abA}
Phenolics and related compounds												
Caffeic acid glucoside	n.d	n.d	n.d	2.0 ± 0.6^{aA}	2.3 ± 0.7^{aA}	14 ± 3^{aB}	106 ± 28^{bC}	27 ± 7^{cB}	18 ± 4^{aA}	80 ± 11^{bB}	17 ± 4^{bA}	22 ± 7^{aA}
Chlorogenic acid	31 ± 6^{aB}	4.5 ± 0.6^{bA}	38 ± 8^{cB}	37 ± 12^{abC}	5 ± 2^{bB}	2.3 ± 0.6^{bA}	26 ± 8^{aB}	0.8 ± 0.2^{aA}	1.2 ± 0.4^{aA}	55 ± 9^{bC}	0.6 ± 0.1^{aA}	1.1 ± 0.2^{aB}
Coumaric acid derivative	n.d	n.d	n.d	1.4 ± 0.2^{aA}	n.d	3.6 ± 0.9^{aB}	58 ± 4^{bB}	6 ± 1^{aA}	48 ± 7^{bC}	112 ± 19^{cC}	9 ± 1^{bA}	50 ± 13^{bB}
Coumaric acid hexose	n.d	1.3 ± 0.2^{a}	n.d	3 ± 1^{aA}	8 ± 3^{bB}	262 ± 55^{aC}	2448 ± 388^{bA}	1981 ± 306^{cA}	2226 ± 351^{cA}	2919 ± 374^{bC}	2213 ± 361^{cB}	1299 ± 214^{bA}
Coumaric acid malonyl-hexose I	0.6 ± 0.1^{aA}	n.d	0.7 ± 0.1^{aA}	0.7 ± 0.2^{aA}	n.d	7 ± 2^{bB}	3.2 ± 0.8^{bA}	24 ± 6^{aB}	47 ± 13^{cC}	4.6 ± 0.7^{cA}	27 ± 2^{aB}	45 ± 11^{cC}
Coumaric acid malonyl-hexose II	0.9 ± 0.1^{aA}	1.5 ± 0.3^{aB}	1.3 ± 0.1^{aB}	0.9 ± 0.2^{aA}	1.8 ± 0.6^{aB}	74 ± 21^{bC}	43 ± 12^{bA}	280 ± 72^{bB}	467 ± 96^{cC}	59 ± 10^{bA}	330 ± 47^{bB}	439 ± 74^{cB}
Coumaric acid malonyl-hexose III	0.6 ± 0.2^{aA}	n.d	0.8 ± 0.2^{aA}	0.8 ± 0.2^{aA}	1.3 ± 0.2^{aB}	29 ± 10^{bC}	10 ± 3^{bA}	92 ± 27^{bB}	176 ± 53^{cC}	15 ± 3^{cA}	84 ± 15^{bB}	133 ± 38^{cC}
Dihydroxybenzoic acid hexose I	17 ± 4^{aB}	8 ± 2^{aA}	61 ± 12^{aC}	17 ± 4^{aB}	6 ± 1^{aA}	51 ± 9^{aC}	17 ± 5^{aB}	8 ± 1^{aA}	59 ± 4^{aC}	20 ± 3^{aB}	8 ± 2^{aA}	55 ± 9^{aC}
Dihydroxybenzoic acid hexose II	14 ± 2^{aB}	10 ± 2^{aA}	66 ± 5^{aC}	16 ± 4^{aB}	7.6 ± 0.7^{aA}	60 ± 10^{aC}	13 ± 4^{aB}	8 ± 1^{aA}	61 ± 5^{aC}	15 ± 3^{aB}	7 ± 2^{aA}	60 ± 8^{aC}
Epicatechin	4 ± 1^{abA}	4 ± 1^{bA}	28 ± 6^{cB}	6 ± 2^{bB}	3 ± 1^{abA}	3 ± 1^{aA}	2.4 ± 0.7^{aB}	0.7 ± 0.2^{aA}	1.7 ± 0.4^{aB}	6 ± 2^{bB}	1.0 ± 0.3^{aA}	6 ± 2^{bB}
Ferulic acid	0.16 ± 0.04^{aA}	n.d	0.17 ± 0.07^{aB}	0.19 ± 0.5^{aA}	0.3 ± 0.1^{aA}	2.3 ± 0.8^{bB}	4 ± 1^{bA}	2.8 ± 0.8^{bA}	9.3 ± 0.9^{cB}	3.1 ± 0.9^{bA}	3.4 ± 0.4^{bA}	8 ± 1^{cB}
Ferulic acid hexose	n.d	n.d	n.d	0.5 ± 0.2^{aA}	0.7 ± 0.2^{aA}	8 ± 3^{aB}	143 ± 25^{cC}	37 ± 11^{bA}	65 ± 18^{bB}	59 ± 17^{bA}	57 ± 13^{bA}	59 ± 14^{bA}
Isotachioside	27 ± 6^{bC}	14 ± 4^{bB}	8 ± 1^{bA}	30 ± 6^{bC}	14 ± 2^{bB}	5.2 ± 0.5^{aA}	16 ± 5^{aC}	9 ± 2^{aB}	5.2 ± 0.7^{aA}	26 ± 3^{bC}	8 ± 1^{aB}	5.0 ± 0.7^{aA}
p-Coumaric acid	n.d	n.d	n.d	n.d	n.d	8 ± 3^{a}	22 ± 5^{aA}	20 ± 4^{aA}	44 ± 12^{bB}	29 ± 5^{aAB}	23 ± 4^{aA}	31 ± 3^{bB}
Tachioside	30 ± 6^{aB}	42 ± 3^{aC}	6 ± 1^{aA}	29 ± 4^{aB}	47 ± 4^{aC}	5.6 ± 0.9^{aA}	25 ± 6^{aB}	43 ± 5^{aC}	7.9 ± 0.4^{bA}	42 ± 5^{bB}	42 ± 4^{aB}	7.5 ± 0.6^{bA}
Phytohormone												
Abscisic acid	0.15 ± 0.04^{aA}	5 ± 2^{aB}	3.7 ± 0.6^{aB}	3 ± 1^{bA}	5.5 ± 0.9^{aB}	7 ± 2^{aB}	8 ± 2^{cA}	11 ± 4^{bAB}	17 ± 1^{cB}	5 ± 1^{bA}	9 ± 3^{bAB}	14 ± 2^{bB}
Vitamin												
Pantothenic acid	18 ± 3^{bB}	12 ± 3^{aA}	11 ± 2^{aA}	15.9 ± 0.9^{abB}	12 ± 2^{aA}	10 ± 2^{aA}	14 ± 2^{aB}	10.5 ± 0.5^{aA}	13 ± 1^{aB}	14 ± 2^{abB}	10 ± 2^{aA}	12 ± 2^{aB}
Not identified metabolites												
Unknown 1 (*m/z* 369)	48 ± 9^{aAB}	38 ± 5^{bA}	55 ± 3^{bB}	46 ± 10^{aA}	39 ± 6^{bA}	36 ± 6^{aA}	38 ± 10^{aA}	26 ± 7^{aA}	32 ± 5^{aA}	53 ± 6^{aC}	24 ± 3^{aA}	39 ± 7^{aB}
Unknown 2 (*m/z* 337)	n.d	n.d	n.d	n.d	n.d	n.d	53 ± 11^{aB}	2.5 ± 0.8^{aA}	2.9 ± 0.7^{aA}	58 ± 12^{aC}	3 ± 1^{aA}	9 ± 2^{bB}
Unknown 3 (*m/z* 381)	722 ± 72^{aB}	5.0 ± 0.6^{aA}	4.9 ± 0.7^{aA}	791 ± 112^{aB}	5.1 ± 0.4^{aA}	6.0 ± 0.7^{aA}	906 ± 211^{abC}	8 ± 2^{bA}	20 ± 4^{bB}	1269 ± 197^{bC}	7.4 ± 0.4^{bA}	31 ± 4^{cB}
Unknown 4 (*m/z* 443)	5 ± 1^{a}	n.d	n.d	7 ± 1^{b}	n.d	n.d	23 ± 6^{cC}	13 ± 5^{aB}	3 ± 1^{aA}	31 ± 9^{cB}	22 ± 3^{bB}	6 ± 2^{bA}
Unknown 5 (*m/z* 391)	28 ± 6^{aB}	n.d	2.2 ± 0.2^{aA}	32 ± 10^{aC}	2.0 ± 0.6^{bA}	3.7 ± 0.7^{bB}	40 ± 13^{aC}	3.0 ± 0.9^{bA}	7 ± 1^{cB}	98 ± 18^{bC}	3 ± 1^{bA}	11 ± 2^{dB}

Data are expressed in mg kg^{-1} dry weight as mean ± standard deviation (n = 5); Different small letters indicate a statistical difference ($p \leq 0.05$) between the ripeness stages of the same variety; Different capital letters indicate a statistical difference ($p \leq 0.05$) at the same ripeness stage between *Bacon*, *Fuerte* and *Hass* varieties; n.d: not detected.

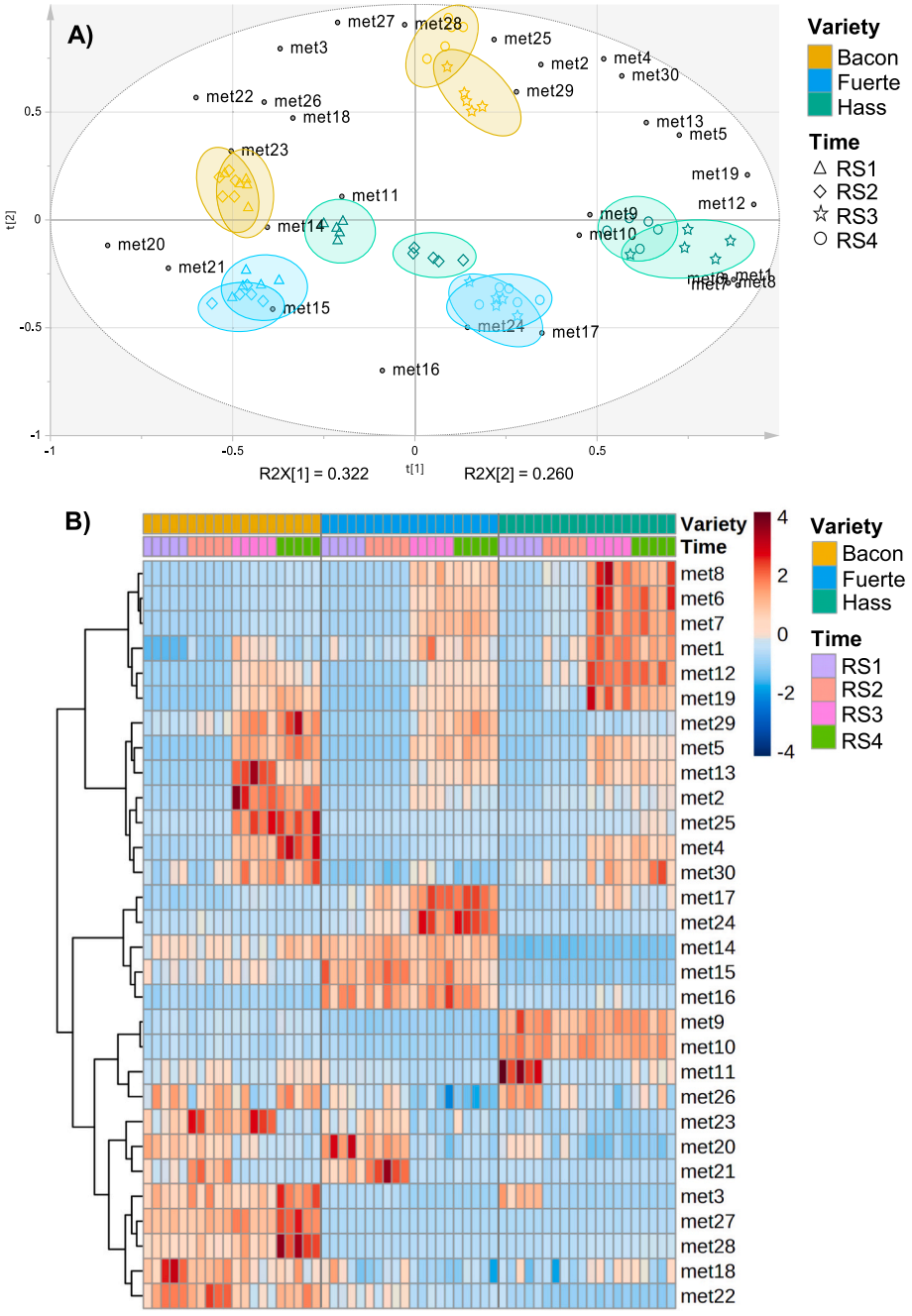

Fig. 1. Two-dimensional (2D) principal component analysis biplot using the first two principal components (**A**) and heat map (**B**) obtained from the LC-MS quantitative data set. Ripening stage: **RS1**- Unripe, **RS2**- Medium, **RS3**- Edible ripeness, **RS4**- Overripe. Meaning of dots: **met1**-Abscisic acid; **met2**- Caffeic acid glucoside, **met3-** Chlorogenic acid, **met4-** Coumaric acid derivative, **met5-** Coumaric acid hexose, **met6-** Coumaric acid malonyl-hexose I, **met7-** Coumaric acid malonyl-hexose Il, **met8-** Coumaric acid malonyl-hexose III, **met9-** Dihydroxybenzoic acid hexose I, **met10-** Dihydroxybenzoic acid hexose II, **met11-** Epicatechin, **met12-** Ferulic acid, **met13-** Ferulic acid hexose, **met14-** Tachioside, **met15-** *N*-acetyl-phenylalanine, **met16-** *N*-acetyl-tryptophan, **met17-** *N*-acetyl-tyrosine, **met18-** Pantothenic acid, **met19-** *p*-Coumaric acid, **met20-** Penstemide, **met21-** Phenylalanine, **met22-** Isotachioside, **met23-** Tryptophan, **met24-** Tyrosine, **met25-** Unknown 2 *(m/z* 337), **met26-** Unknown 1 (*m/z* 369), **met27**- Unknown 3 *(m/z* 381), **met28-** Unknown 5 *(m/z* 391), **met29-** Unknown 4 *(m/z* 443), **met30-** Uridine.

not seem to be directly correlated with ripening phenomena, they do play a significant role in distinguishing varietal characteristics. The concentration found in *Hass* avocados was three times higher (ranging from 51 to 61 mg kg^{-1} DW) than in *Bacon* and *Fuerte* varieties at all ripening stages.

Moving beyond this specific compound, most other phenolic compounds (elaborated upon later) exhibited a significant ($p \leq 0.05$) increase in content during fruit softening. Several showed a steady increase from RS1 to RS4, while others progressively increased from RS1 to RS3 and subsequently decreased with senescence, though not always significantly. This latter pattern was particularly evident in *Hass* avocados. This trend aligns with the findings of Villa-Rodríguez et al. (2011), who reported the highest total phenolic content in mature fruit and the lowest in unripe fruit for *Hass* avocados. The authors also emphasised the negative impact of the senescence stage on the phenolic content of *Hass* avocados. Similarly, Zhang et al. (2013) documented a trend of total phenolic accumulation during ripening in the avocado cv. *Booth 7*. It is essential to take into account the large number of

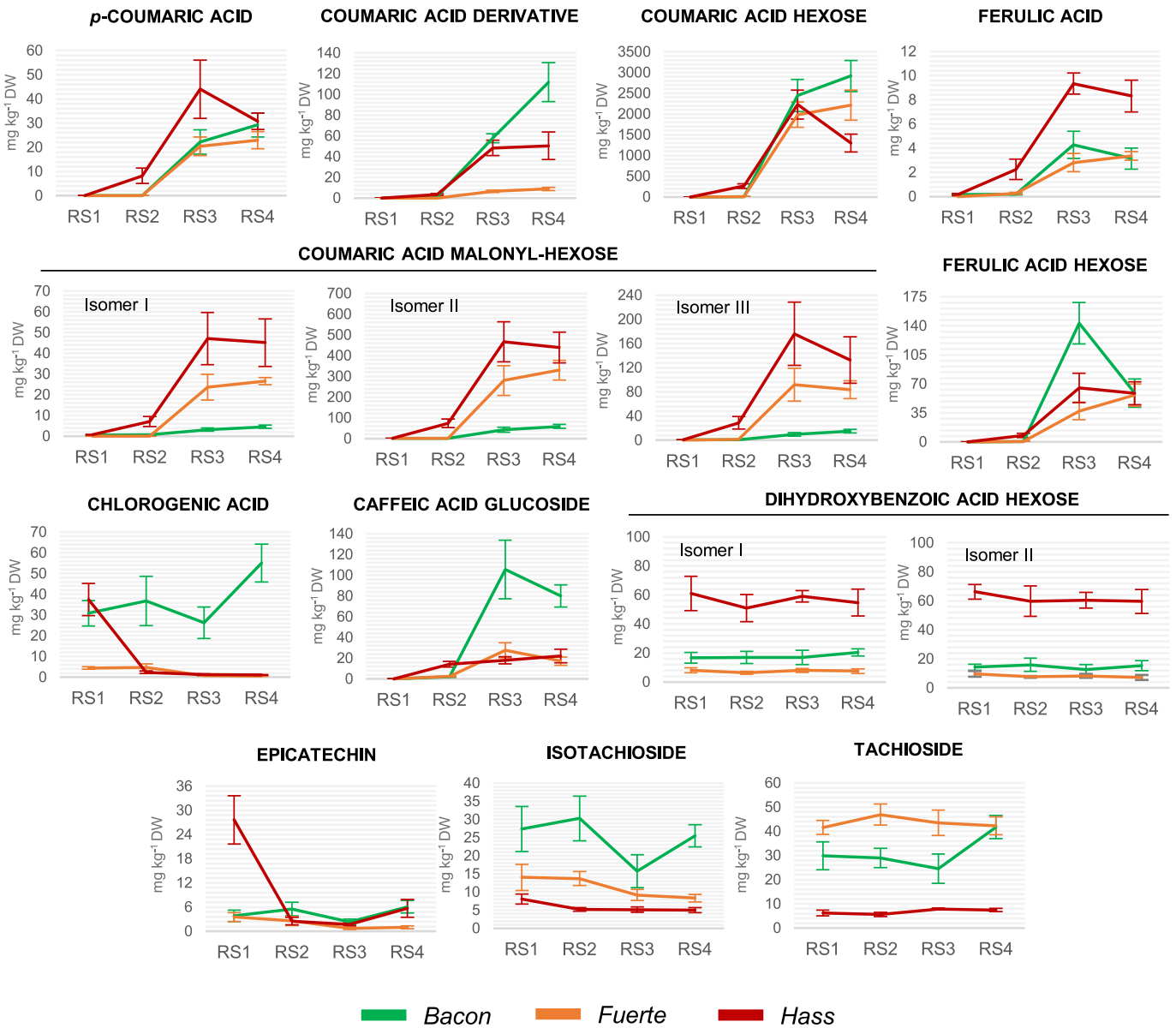

Fig. 2. Graphical depictions of individual trends observed during ripening for the fifteen phenolic compounds and related substances determined in the avocado pulp of *Hass*, *Fuerte* and *Bacon* samples.

metabolites that are quantified individually in this work; no such research has been carried out so comprehensively so far, only a rather partial comparison with literature results will be possible.

The overall increase of many phenolic compounds during fruit softening would be related to the enzyme phenylalanine ammonia lyase (PAL), which is one of the key players in the initiation of phenolic biosynthesis. This pivotal enzyme operates within the phenylpropanoid pathway of plant metabolism and is responsible for catalysing the deamination of phenylalanine, leading to the formation of *trans*-cinnamic acid (Bajguz & Piotrowska-Niczyporuk, 2023). PAL activity is subject to stresses and increases as part of a plant defence response against diseases, insect attacks, and the stress commonly encountered by many fleshy fruits during ripening (Bajguz & Piotrowska-Niczyporuk, 2023; Tomás-Barberán & Espín, 2001). Indeed, fruit softening is a clear way to increase fruit vulnerability. Moreover, the induction of PAL activity by ethylene has been suggested on several occasions (Li et al., 2022; Tomás-Barberán & Espín, 2001), which is particularly relevant in climacteric fruits such as avocado.

Looking deeper into the individual phenolic metabolites shown in Fig. 2, *p*-coumaric and ferulic acids (two simple hydroxycinnamic acids), showed a significant increase in concentration ($p \leq 0.05$) as the avocado ripened. Previous reports have described these same trends (Contreras-Gutiérrez et al., 2013; Di Stefano et al., 2017; Hurtado-Fernández et al., 2011, 2014). Within the phenolic compounds category, the most substantial concentrations were observed for compounds derived from coumaric acid. Notably, all these compounds exhibited a parallel increase in concentration as the fruit ripened, at least up to the ready-to-eat stage (RS3). Several coumaric acid derivatives have been previously described by Pedreschi et al. (2022) who also observed the described increase as the avocado fruit ripened.

Despite a common general trend, certain varietal differences were observed. For example, even though the isomer II of coumaric acid malonyl-hexose was the most abundant in all three varieties, its evolution was much less pronounced in *Bacon* than in *Hass* and *Fuerte*. Something similar occurred with the coumaric acid derivative in *Fuerte* fruits, which exhibited a less pronounced increase compared to *Bacon*

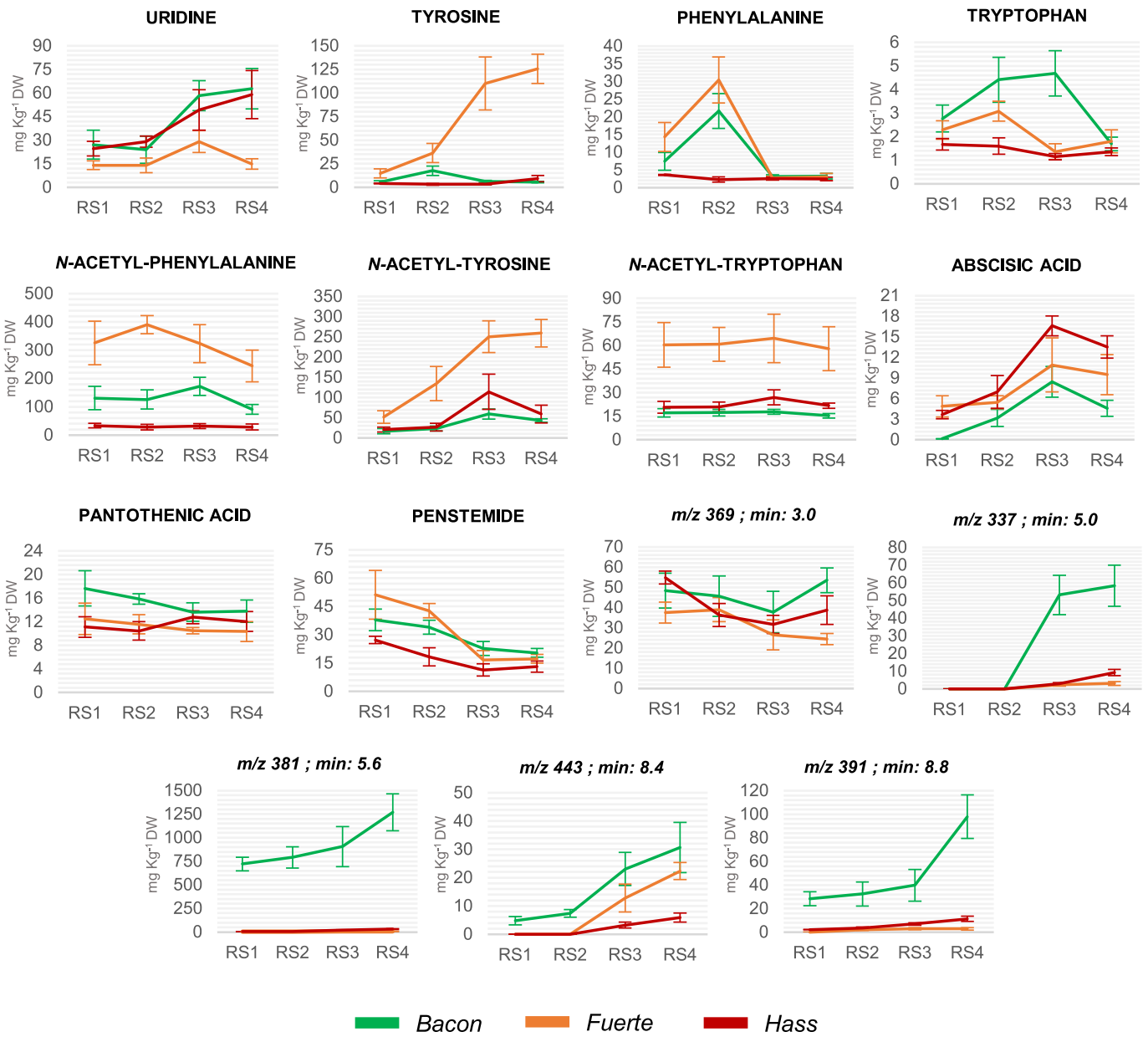

Fig. 3. Quantitative evolution patterns observed over ripening for amino acids, nucleosides and related compounds, iridoids, phytohormones, vitamins, and the five not fully annotated substances determined in the avocado pulp of *Hass*, *Fuerte* and *Bacon* varieties.

avocados. The coumaric acid hexose, which was the most predominant compound, evolved in a rather similar way and with a very comparable content regardless of the variety up to the ready-to-eat stage. From that point onwards, the levels found in ripe avocados were maintained in *Bacon* and *Fuerte* fruits (even showing a slight increase), while in *Hass* it decreased significantly in the overripe stage.

The remaining glycosidic forms of phenolic acids, namely ferulic acid hexose and caffeic acid glucoside, exhibited dominance in *Bacon* (compared to the other varieties) as the fruit ripened, although the observed increase was shared across all varieties. Specifically, ferulic acid hexose in *Bacon* reached its peak only up to the edible ripeness, but experienced a significant decline, reaching mean values comparable to the other two varieties (57–59 mg kg^{-1} DW) in the post-climacteric stage. In contrast, the decrease of caffeic acid glucoside in *Bacon* at overripe fruits was less pronounced and did not reach statistical significance. As previously highlighted, the rate at which metabolic changes unfolded within each fruit was a significant differentiator between the varieties tested.

Chlorogenic acid showed a distinctive evolution depending on the variety observed. For example, cv. *Bacon* and *Hass* showed similar concentrations in unripe avocados (RS1) with 31 ± 6 and 38 ± 8 mg kg^{-1} DW, respectively. However, a significant decrease in the concentration of this compound in RS2 characterised *Hass* fruits. This is similar to what was also observed by Di Stefano et al. (2017) and Hurtado-Fernández et al. (2011, 2014). Di Stefano et al. (2017) also studied *Bacon* and *Fuerte* varieties, describing a decrease in chlorogenic acid in *Bacon* and an increase in *Fuerte* from unripe to ripe fruit (considering only 2 ripening stages). In this research, chlorogenic acid in *Fuerte* showed a quantitative evolution comparable to *Hass*, although with lower overall values. However, in avocados cv. *Bacon*, the concentration of this compound was maintained or even increased significantly as they matured, with contents of up to 55 mg kg^{-1} DW in the overripe stage. This distinctive characteristic of high chlorogenic acid contents in *Bacon* fruits aligns with findings by Hurtado-Fernández et al. (2016), who exclusively analysed ripe avocados from several varieties. It is noteworthy that although chlorogenic acid was determined in all studied

samples, its accumulation predominantly occurs in the avocado peel rather than the pulp (Beiro-Valenzuela et al., 2023; Ramos-Aguilar et al., 2021).

Epicatechin showed a decrease in *Hass* avocados, particularly from early to medium ripeness. Its concentration also decreased overall in *Fuerte* and exhibited some fluctuations in *Bacon*. This reduction from green to ripe *Hass* fruit is in agreement with data reported by Hurtado-Fernández et al. (2011). Also Di Stefano et al. (2017) observed a decreasing trend of epicatechin with fruit ripening (for all the varieties they studied except *Hass*). Villa-Rodriguez et al. (2020) reported that epicatechin reached its maximum contents in RS4, finding 126.6 mg kg^{-1} for *Hass* samples from Mexico, a value significantly higher than those determined for the samples considered in this work. The highest observed concentrations of this flavon-3-ol were 28 ± 6 mg kg^{-1} DW, found in the green *Hass* fruit (RS1). Epicatechin is involved in the regulation of the lipoxygenase activity in avocado, making it an important factor in modulating the fruit's resistance to post-harvest attack (Guetsky et al., 2005). Epicatechin is additionally associated with the browning of mesocarp tissue (Tesfay et al., 2011). Finally, both peaks, tentatively identified as isotachioside and tachioside (glycosidic phenols), showed a closer similarity to the glycosidic isomers of dihydroxybenzoic acid. Although significant differences were detected during ripening in both *Bacon* and *Hass* varieties, no pronounced overall trend was observed. Both substances exhibited notable concentrations in RS1 and RS2 avocados; for instance, in RS1 for *Bacon* isotachioside and tachioside, respectively, were found at 27 ± 6 and 30 ± 6 mg kg^{-1} DW, and in *Fuerte* the concentration levels were 14 ± 4 and 42 ± 3 mg kg^{-1} DW, for the same analytes.

3.2.2.2. Quantitative progression of the remaining considered metabolites (amino acids and related compounds, nucleosides, iridoids, phytohormones, vitamins, and unidentified substances). Plant amino acid metabolism plays a fundamental role, serving as the basis for protein synthesis, respiration processes and the synthesis of various other metabolites (Pedreschi et al., 2019). For instance, phenylalanine is the primary precursor in the phenylpropanoid biosynthesis pathway. In addition, free amino acids are important for the synthesis or enhanced activity of several enzymes that operate during climacteric ripening. Amino acids and derivatives can also influence fruit aroma, taste an quality (Mandrioli et al., 2013). While avocado fruit is relatively rich in protein, the role of free amino acids in postharvest avocado ripening has received minimal attention over the years. Significant differences were observed in both variety and ripeness stage for the amino acids and *N*-acetyl-amino acid derivatives group, although a discernible general pattern could not be defined. In contrast to phenolic compounds, the individual trends within this group exhibited a high level of heterogeneity.

In terms of total amino acids and derivatives contents, *Fuerte* fruits consistently exhibited the highest amounts, both in green and ripe avocados, while *Hass* fruits displayed the lowest contents. *Bacon* fruits showed significantly higher levels of tryptophan concentration exclusively. Examining the individual compounds of this category (Fig. 3), the steadiest evolution was observed for tyrosine and *N*-acetyl-tyrosine levels, which underwent a strong increase, particularly in *Fuerte*. Tyrosine levels in *Fuerte* at RS4 were 126 ± 6 mg kg^{-1} DW and *N*-acetyl-tyrosine levels were 259 ± 34 mg kg^{-1} DW, respectively. The distinct increasing trend observed was not replicated in *Hass* and *Bacon* varieties, although a partial resemblance was noted for *N*-acetyl-tyrosine, albeit to a lesser extent.

Phenylalanine exhibited a positive evolution in the early stages of climacteric ripening in *Fuerte* and *Bacon*, with a notable reduction upon reaching maturity for consumption. In contrast, *Hass* fruits showed a minimal reduction over time. Tryptophan increased significantly ($p \leq 0.05$) in *Bacon* fruits during climacteric ripening, rising from 2.8 ± 0.6 to 5 ± 1 mg kg^{-1} DW, with the highest levels reached at the edible ripeness stage. This metabolite did not show significant and consistent changes in *Hass* and *Fuerte*. There were no significant changes in the contents of *N*-acetyl-tryptophan for any of the varieties analysed. Although there were alterations in the levels of *N*-acetyl-phenylalanine in *Bacon* and *Fuerte*, the progression was not distinctly evident. In *Fuerte* fruits, both metabolites stood out, implying that they could potentially serve as specific markers for this cultivar, as previously mentioned. The cultivar-dependent behaviour of amino acids and derivatives may be associated with the unique requirements of each variety, as these compounds are essential for providing foundational components necessary for protein synthesis, respiration, and the biosynthesis of various secondary metabolites.

Regarding nucleosides, we observed consistently elevated and statistically significant ($p \leq 0.05$) levels of uridine as fruits ripened across all three varieties. Notably, in the case of *Fuerte*, a distinct and significant decline was observed as it approached senescence. Nucleosides serve as crucial precursors for nucleotide synthesis, which in turn are fundamental building blocks of nucleic acids like DNA and RNA. These molecules play pivotal roles in the storage, transfer, and expression of genetic information (Domínguez-Álvarez et al., 2017). It is documented that in avocado fruit, the expression of numerous genes undergoes alterations through ripening under the influence of the phytohormone ethylene (McGarvey et al., 1992). Therefore, if the number of specific mRNAs increased with ripening, the documented rise in uridine as fruit ripened could be consequence of the increased demand for precursors.

Penstemide, identified as the only iridoid compound, showed a steady decline in all varieties, reaching its highest levels in green fruit and dropping to the lowest levels at the overripe stage. Iridoids are secondary plant metabolites and comprise the predominant category of monoterpenoids with acyclopentan-[C]-pyran skeleton. Even though cytotoxic properties have been attributed to penstemide (Wysokinska et al., 1992), there are currently no available reports providing evidence of the impact of iridoids on the climacteric ripening process of fruits.

Pantothenic acid (a water-soluble B_5-vitamin) is the main precursor for the biosynthesis of coenzyme A (CoA) which is an essential cofactor for the respiratory pathway but also plays a key role in fatty acid synthesis/oxidation and the synthesis of many secondary metabolites (Webb et al., 2004). Nevertheless, this metabolite showed a minimal significant reduction in *Bacon* during fruit ripening, remained stable in *Fuerte*, and showed irregular fluctuations in *Hass* without a discernible pattern. Considering these results, pantothenic acid content would not be correlated with the climacteric ripening, despite its role in supporting concurrent biosynthetic pathways. Interestingly, Serrano-García et al. (2022) observed that this vitamin was also not altered by a prolonged on tree fruit maturation or storage in cold chambers, although displayed comparable ranges (9–15 mg kg^{-1} DW) to those observed in the present study for *Hass* fruits at edible ripeness.

Abscisic acid (ABA) demonstrated consistent behaviour throughout the study. A progressive increase in ABA content was observed in the avocado fruit mesocarp during softening, mirroring a similar pattern to ethylene biosynthesis and the respiration rate up to a specific threshold. In all three varieties studied, the highest ABA concentration in the pulp occurred just after the climacteric peak at RS3, with values ranging from 8 to 17 mg kg^{-1} DW depending on the cultivar. Subsequently, ABA levels declined with senescence. Slightly higher ready-to-eat ABA values of 19.6–26.8 mg kg^{-1} DW were reported by Chirinos et al. (2021) for *Hass* fruits obtained at different harvest dates and subjected to different storage conditions; the small differences observed could be related to variations in maturation rates and overall shelf life. Previous results have already suggested a link between ABA and ethylene metabolism (Meyer et al., 2017). In fact, recent developments seem to indicate that the ripening of climacteric fruits is not only due to ethylene, but to an interaction with other phytohormones, so that ABA, auxin, jasmonates, brassinosteroids and cytokinins may act as signalling molecules that stimulate the ripening of these climacteric fruits by inducing the expression of ripening-related genes (Vincent et al., 2020). At the molecular level, the biosynthetic pathway of ABA in plants typically

incorporates carotenoids as precursors, leading to the production of xanthoxin. Subsequently, xanthoxin is converted into ABA-aldehyde, and further transformation results in ABA, which represents the biologically active form of the hormone. Indeed, the impact of ripening on carotenoid content in avocado pulp has been previously documented with a consistent reduction, a fact that could be partially attributed to the requirement of carotenoids for ABA synthesis (Ashton et al., 2006; Villa-Rodriguez et al., 2020).

As previously highlighted, unknowns 2, 3 and 5 at m/z 337, 381, and 391 appear distinctly associated with *Bacon* fruits, exhibiting significantly higher concentrations in this variety regardless of the ripening stage. Notably, in *Bacon* avocados, the concentration of these compounds increases with ripeness, although a minor elevation on a different concentration scale is also observed in the other two varieties. A similar, albeit less pronounced, trend is observed for the unknown 4 (m/z 443), with its concentration displaying a comparable increase across all three varieties. Conversely, the concentration of the unidentified compound with m/z 369 remained relatively unchanged in *Bacon* but decreased significantly ($p \leq 0.05$) in *Hass* and *Fuerte* as the fruits ripened. Considering the demonstrated relevance of these substances, especially in distinguishing the *Bacon* variety, it is imperative to further investigate and elucidate their structure, ultimately assigning them a name. Ongoing analyses in this direction are currently being conducted in our laboratory.

4. Conclusions

A powerful LC-MS method has been applied to quantify thirty relevant individual metabolites throughout the entire avocado ripening process, spanning from unripe to overripe stages, in three commercially significant avocado varieties (*Hass*, *Fuerte*, and *Bacon*). The aim was to explore the dynamic metabolic transformations occurring during ripening, while considering the influence of the variety. Noteworthy metabolic differences were observed between unripe and ripe fruits, as well as among the evaluated genotypes. The phenolic compound group exhibited a consistent increase over time during ripening, while the behaviour of amino acids and related compounds was predominantly cultivar dependent. Abscisic acid, uridine, and penstemide displayed consistent trends across all three varieties. Additionally, the abundance of several unidentified compounds was found to be characteristic of the *Bacon* variety, with these analytes showing an increase with fruit ripening. Future research efforts integrating multi-omics methods will provide a more comprehensive understanding of the physicochemical processes underlying avocado ripening dynamics. This work, along with future studies, aims to deepen our insight into the biosynthetic pathways of key metabolites and their variation among commercially available avocado cultivars.

Funding sources

This research has been partially financed by Grants PID2021-128508OB-I00 and PID2022-141851OB-I00 funded by MCIN/AEI/10.13039/501100011033 and "FEDER Una manera de hacer Europa", by Grant PID2019-109566RB-I00 funded by MCIN/AEI /10.13039/501100011033, and the Millennium Science Initiative Program – ICN2021_044. Authors are grateful for the financial support received from the Spanish Government (FPU19/00700) (I·S-G.), and from "UE-NextGenerationUE" (R.P.M.). Funding for open access charge: Universidad de Granada / CBUA.

CRediT authorship contribution statement

Irene Serrano-García: Writing – review & editing, Writing – original draft, Methodology, Investigation, Formal analysis, Data curation. **Carlos Saavedra Morillas:** Methodology, Investigation, Formal analysis, Data curation. **María Gemma Beiro-Valenzuela:** Writing – review & editing, Methodology, Formal analysis, Data curation. **Romina Monasterio:** Writing – review & editing, Methodology, Formal analysis, Data curation. **Elena Hurtado-Fernández:** Writing – review & editing, Methodology, Formal analysis, Data curation. **José Jorge González-Fernández:** Writing – review & editing, Resources, Funding acquisition, Conceptualization. **José Ignacio Hormaza:** Writing – review & editing, Resources, Funding acquisition, Conceptualization. **Romina Pedreschi:** Writing – review & editing, Resources, Funding acquisition, Data curation. **Lucía Olmo-García:** Writing – review & editing, Resources, Funding acquisition, Conceptualization. **Alegría Carrasco-Pancorbo:** Writing – review & editing, Writing – original draft, Supervision, Resources, Project administration, Methodology, Investigation, Funding acquisition, Conceptualization.

Declaration of competing interest

The authors declare that they have no known competing financial interests or personal relationships that could have appeared to influence the work reported in this paper.

Data availability

Data will be made available on request.

Appendix A. Supplementary data

Supplementary data to this article can be found online at https://doi.org/10.1016/j.foodchem.2024.140334.

References

AOAC. (2016). Association of Official Analytical Chemists. In *Official methods of analysis of AOAC international* (20th ed.). Latimer G.W.

Ashton, O. B. O., Wong, M., McGhie, T. K., Vather, R., Wang, Y., Requejo-Jackman, C., … Woolf, A. B. (2006). Pigments in avocado tissue and oil. *Journal of Agricultural and Food Chemistry, 54*(26), 10151–10158. https://doi.org/10.1021/jf061809j

Babiker, E. E., Mohamed Ahmed, I. A., Uslu, N., Özcan, M. M., Al Juhaimi, F., Ghafoor, K., & Almusallam, I. A. (2021). Influence of drying methods on bioactive properties, fatty acids and phenolic compounds of different parts of ripe and unripe avocado fruits. *Journal of Oleo Science, 70*(4), 589–598. https://doi.org/10.5650/jos.ess20343

Bajguz, A., & Piotrowska-Niczyporuk, A. (2023). Biosynthetic pathways of hormones in plants. *Metabolites, 13*, 1–36. https://doi.org/10.3390/metabo13080884

Balasundram, N., Sundram, K., & Samman, S. (2006). Phenolic compounds in plants and agri-industrial by-products: Antioxidant activity, occurrence, and potential uses. *Food Chemistry, 99*, 191–203. https://doi.org/10.1016/j.foodchem.2005.07.042

Beiro-Valenzuela, M. G., Serrano-García, I., Monasterio, R. P., Moreno-Tovar, M. V., Hurtado-Fernández, E., González-Fernández, J. J., … Carrasco-Pancorbo, A. (2023). Characterization of the polar profile of bacon and fuerte avocado fruits by hydrophilic interaction liquid chromatography-mass spectrometry: Distribution of non-structural carbohydrates, quinic acid, and chlorogenic acid between seed, Mesocarp, and exocar. *Journal of Agricultural and Food Chemistry, 71*, 5674–5685. https://doi.org/10.1021/acs.jafc.2c08855

Blakey, R. J., Tesfay, S. Z., Bertling, I., & Bower, J. P. (2012). Changes in sugars, total protein, and oil in "Hass" avocado (*Persea americana* Mill.) fruit during ripening. *Journal of Horticultural Science and Biotechnology, 87*(4), 381–387. https://doi.org/10.1080/14620316.2012.11512880

Campos, D., Teran-Hilares, F., Chirinos, R., Aguilar-Galvez, A., García-Ríos, D., Pacheco-Avalos, A., & Pedreschi, R. (2020). Bioactive compounds and antioxidant activity from harvest to edible ripeness of avocado cv. Hass (*Persea americana*) throughout the harvest seasons. *International Journal of Food Science and Technology, 55*, 2208–2218. https://doi.org/10.1111/ijfs.14474

Cascallar, E. C. (2020). 1.2 El aguacate en la Península Ibérica. In A. Namesny, C. Conesa, I. Hormaza, & G. Lobo (Eds.), *Cultivo, Poscosecha y Procesado Del Aguacate* (pp. 19–26).

Chirinos, R., Campos, D., Martinez, S., Llanos, S., Betalleluz-Pallardel, I., García-Ríos, D., & Pedreschi, R. (2021). The effect of hydrothermal treatment on metabolite composition of Hass avocados stored in a. *Plants, 10*, 2427. https://doi.org/10.3390/plants10112427

Contreras-Gutiérrez, P. K., Hurtado-Fernández, E., Gómez-Romero, M., Hormaza, J. I., Carrasco-Pancorbo, A., & Fernández-Gutiérrez, A. (2013). Determination of changes in the metabolic profile of avocado fruits (*Persea americana*) by two CE-MS approaches (targeted and non-targeted). *Electrophoresis, 34*(19), 2928–2942. https://doi.org/10.1002/elps.201200676

Cowan, A. K. (2004). Metabolic control of avocado fruit growth: 3-hydroxy-3-methylglutaryl coenzyme a reductase, active oxygen species and the role of C7 sugars. *South*

African Journal of Botany, 70(1), 75–82. https://doi.org/10.1016/S0254-6299(15)30309-4

Crane, J. H., Douhan, G., Faber, B. A., Arpaia, M. L., Bender, G. S., Balerdi, C. F., & Barrientos-Priego, A. F. (2013). Cultivars and rootstocks. In B. Schaffer, B. N. Wolstenholme, & A. W. Whiley (Eds.), *The avocado: Botany, production and uses* (2nd Editio, pp. 200–233). CAB International. https://doi.org/10.1079/9781845937010.0200.

Defilippi, B. G., Ejsmentewicz, T., Covarrubias, M. P., Gudenschwager, O., & Campos-Vargas, R. (2018). Changes in cell wall pectins and their relation to postharvest mesocarp softening of "Hass" avocados (*Persea americana* Mill.). *Plant Physiology and Biochemistry, 128*(May), 142–151. https://doi.org/10.1016/j.plaphy.2018.05.018

Di Stefano, V., Avellone, G., Bongiorno, D., Indelicato, S., Massenti, R., & Lo Bianco, R. (2017). Quantitative evaluation of the phenolic profile in fruits of six avocado (*Persea americana*) cultivars by ultra-high-performance liquid chromatography-heated electrospray-mass spectrometry. *International Journal of Food Properties, 20*(6), 1302–1312. https://doi.org/10.1080/10942912.2016.1208225

Domínguez-Álvarez, J., Mateos-Vivas, M., Rodríguez-Gonzalo, E., García-Gómez, D., Bustamante-Rangel, M., Delgado Zamarreño, M. M., & Carabias-Martínez, R. (2017). Determination of nucleosides and nucleotides in food samples by using liquid chromatography and capillary electrophoresis. *TrAC, Trends in Analytical Chemistry, 92*, 12–31. https://doi.org/10.1016/j.trac.2017.04.005

FAO. (2023). *FAOSTAT*. Statistics Division of Food and Agriculture Organization of the United Nations. https://www.fao.org/faostat/en/#home.

Gómez-Maqueo, A., Escobedo-Avellaneda, Z., & Welti-Chanes, J. (2020). Phenolic compounds in mesoamerican fruits—Characterization, health potential and processing with innovative technologies. *International Journal of Molecular Sciences, 21*(21), 1–41. https://doi.org/10.3390/ijms21218357

Guetsky, R., Kobiler, I., Wang, X., Perlman, N., Gollop, N., Avila-Quezada, G., Hadar, I., & Prusky, D. (2005). Metabolism of the flavonoid epicatechin by laccase of Colletotrichum gloeosporioides and its effect on pathogenicity on avocado fruits. *Phytopathology, 95*(11), 1341–1348. https://doi.org/10.1094/PHYTO-95-1341

Hurtado-Fernandez, E., Fernandez-Gutierrez, A., & Carrasco-Pancorbo, A. (2016). Avocado fruit—Persea americana. In S. Rodrigues, E.d. O. Silva, & E. S. de Brito (Eds.), *Exotic fruits reference guide* (pp. 37–48). https://doi.org/10.1016/B978-0-12-803138-4.00001-0

Hurtado-Fernández, E., Pacchiarotta, T., Mayboroda, O. A., Fernández-Gutiérrez, A., & Carrasco-Pancorbo, A. (2015). Metabolomic analysis of avocado fruits by GC-APCI-TOF MS: Effects of ripening degrees and fruit varieties. *Analytical and Bioanalytical Chemistry, 407*, 547–555. https://doi.org/10.1007/s00216-014-8283-9

Hurtado-Fernández, E., González-Fernández, J. J., Hormaza, J. I., Bajoub, A., Fernández-Gutiérrez, A., & Carrasco-Pancorbo, A. (2016). Targeted LC-MS approach to study the evolution over the harvesting season of six important metabolites in fruits from different avocado cultivars. *Food Analytical Methods, 9*, 3479–3491. https://doi.org/10.1007/s12161-016-0523-5

Hurtado-Fernández, E., Pacchiarotta, T., Gómez-Romero, M., Schoenmaker, B., Derks, R., Deelder, A. M., … Fernández-Gutiérrez, A. (2011). Ultra high performance liquid chromatography-time of flight mass spectrometry for analysis of avocado fruit metabolites: Method evaluation and applicability to the analysis of ripening degrees. *Journal of Chromatography A, 1218*(42), 7723–7738. https://doi.org/10.1016/j.chroma.2011.08.059

Hurtado-Fernández, E., Pacchiarotta, T., Mayboroda, O. A., Fernández-Gutiérrez, A., & Carrasco-Pancorbo, A. (2014). Quantitative characterization of important metabolites of avocado fruit by gas chromatography coupled to different detectors (APCI-TOF MS and FID). *Food Research International, 62*, 801–811. https://doi.org/10.1016/j.foodres.2014.04.038

Kassim, A., Workneh, T. S., & Bezuidenhout, C. N. (2013). A review on postharvest handling of avocado fruit. *African Journal of Agricultural Research, 8*(21), 2385–2402. https://doi.org/10.5897/AJAR12.1248

Li, X., Li, B., Li, M., Fu, X., Zhao, X., Min, D., Li, F., & Zhang, X. (2022). Ethylene pretreatment induces phenolic biosynthesis of fresh-cut pitaya fruit by regulating ethylene signaling pathway. *Postharvest Biology and Technology, 192*(July), Article 112028. https://doi.org/10.1016/j.postharvbio.2022.112028

Lin, D., Xiao, M., Zhao, J., Li, Z., Xing, B., Li, X., Kong, M., Li, L., Zhang, Q., Liu, Y., Chen, H., Qin, W., Wu, H., & Chen, S. (2016). An overview of plant phenolic compounds and their importance in human nutrition and management of type 2 diabetes. *Molecules, 21*, 1374. https://doi.org/10.3390/molecules21101374

López-Cobo, A., Gómez-Caravaca, A. M., Pasini, F., Caboni, M. F., Segura-Carretero, A., & Fernández-Gutiérrez, A. (2016). HPLC-DAD-ESI-QTOF-MS and HPLC-FLD-MS as valuable tools for the determination of phenolic and other polar compounds in the edible part and by-products of avocado. *LWT - Food Science and Technology, 73*, 505–513. https://doi.org/10.1016/j.lwt.2016.06.049

Mandrioli, R., Mercolini, L., & Raggi, M. A. (2013). Recent trends in the analysis of amino acids in fruits and derived foodstuffs. *Analytical and Bioanalytical Chemistry, 405*, 7941–7956. https://doi.org/10.1007/s00216-013-7025-8

McGarvey, D. J., Sirevåg, R., & Christoffersen, R. E. (1992). Ripening-related gene from avocado fruit: Ethylene-inducible expression of the mRNA and polypeptide. *Plant Physiology, 98*, 554–559. https://doi.org/10.1104/pp.98.2.554

Meyer, M. D., Chope, G. A., & Terry, L. A. (2017). Investigation into the role of endogenous abscisic acid during ripening of imported avocado cv. Hass. *Journal of the Science of Food and Agriculture, 97*(11), 3656–3664. https://doi.org/10.1002/jsfa.8225

Núñez-Lillo, G., Ponce, E., Arancibia-Guerra, C., Carpentier, S., Carrasco-Pancorbo, A., Olmo-García, L., Chirinos, R., Campos, D., Campos-Vargas, R., Meneses, C., & Pedreschi, R. (2023). A multiomics integrative analysis of color de-synchronization with softening of 'Hass' avocado fruit: A first insight into a complex physiological disorder. *Food Chemistry, 408*(December 2022). https://doi.org/10.1016/j.foodchem.2022.135215

Pedreschi, R., Ponce, E., Hernández, I., Fuentealba, C., Urbina, A., González-Fernández, J. J., … Aguayo, E. (2022). Short vs. long-distance avocado supply chains: Life cycle assessment impact associated to transport and effect of fruit origin and supply conditions chain on primary and secondary metabolites. *Foods, 11*, 1807. https://doi.org/10.3390/foods11121807

Pedreschi, R., Uarrota, V., Fuentealba, C., Alvaro, J. E., Olmedo, P., Defilippi, B. G., … Campos-Vargas, R. (2019). Primary metabolism in avocado fruit. *Frontiers in Plant Science, 10*, 795. https://doi.org/10.3389/fpls.2019.00795

Ramos-Aguilar, A. L., Ornelas-Paz, J., Tapia-Vargas, L. M., Gardea-Bejar, A. A., Yahia, E. M., Ornelas-Paz, J.d. J., … Escalante-Minakata, P. (2021). Metabolomic analysis and physical attributes of ripe fruits from Mexican Creole (*Persea americana var. drymifolia*) and "Hass" avocados. *Food Chemistry, 354*. https://doi.org/10.1016/j.foodchem.2021.129571

Ruttkies, C., Schymanski, E. L., Wolf, S., Hollender, J., & Neumann, S. (2016). MetFrag relaunched: Incorporating strategies beyond in silico fragmentation. *Journal of Cheminformatics, 8*, 3. https://doi.org/10.1186/s13321-016-0115-9

Serrano-García, I., Dominguez-García, J., Hurtado-Fernandez, E., González-Fernández, J. J., Hormaza, I., Beiro-Valenzuela, M. G., … Carrasco-Pancorbo, A. (2023). Assessing the RP-LC-MS-based metabolic profile of Hass avocados marketed in Europe from different geographical origins (Peru, Chile, and Spain) over the whole season. *Plants, 12*, 3004. https://doi.org/10.3390/plants12163004

Serrano-García, I., Hurtado-Fernández, E., Gonzalez-Fernandez, J. J., Hormaza, J. I., Pedreschi, R., Reboredo-Rodríguez, P., … Carrasco-Pancorbo, A. (2022). Prolonged on-tree maturation vs. cold storage of Hass avocado fruit: Changes in metabolites of bioactive interest at edible ripeness. *Food Chemistry, 394*(December 2021). https://doi.org/10.1016/j.foodchem.2022.133447

Talavera, A., Gonzalez-Fernandez, J. J., Carrasco-Pancorbo, A., Olmo-García, L., & Hormaza, J. (2023). Avocado: Agricultural Importance and Nutraceutical Properties. In C. Kole (Ed.), *Compendium of crop genome designing for nutraceuticals* (1st Editio, pp. 1–19). Springer Singapore. https://doi.org/10.1007/978-981-19-3627-2.

Tesfay, S. Z., Bertling, I., & Bower, J. P. (2010). Anti-oxidant levels in various tissues during the maturation of "Hass" avocado (*Persea americana* Mill.). *Journal of Horticultural Science and Biotechnology, 85*(2), 106–112. https://doi.org/10.1080/14620316.2010.11512639

Tesfay, S. Z., Bertling, I., & Bower, J. P. (2011). Seasonal trends of specific phenols in "Hass" avocado tissues. *Acta Horticulturae, 911*, 349–354. https://doi.org/10.17660/ActaHortic.2011.911.40

Tesfay, S. Z., Bertling, I., & Bower, J. P. (2012). D-mannoheptulose and perseitol in "Hass" avocado: Metabolism in seed and mesocarp tissue. *South African Journal of Botany, 79*, 159–165. https://doi.org/10.1016/j.sajb.2011.10.006

Tomás-Barberán, F. A., & Espín, J. C. (2001). Phenolic compounds and related enzymes as determinants of quality in fruits and vegetables. *Journal of the Science of Food and Agriculture, 81*, 853–876. https://doi.org/10.1002/jsfa.885

Villa-Rodríguez, J. A., Molina-Corral, F. J., Ayala-Zavala, J. F., Olivas, G. I., & González-Aguilar, G. A. (2011). Effect of maturity stage on the content of fatty acids and antioxidant activity of "Hass" avocado. *Food Research International, 44*(5), 1231–1237. https://doi.org/10.1016/j.foodres.2010.11.012

Villa-Rodriguez, J. A., Yahia, E. M., González-León, A., Ifie, I., Robles-Zepeda, R. E., Domínguez-Avila, J. A., & González-Aguilar, G. A. (2020). Ripening of 'Hass' avocado mesocarp alters its phytochemical profile and the in vitro cytotoxic activity of its methanolic extracts. *South African Journal of Botany, 128*, 1–8. https://doi.org/10.1016/j.sajb.2019.09.020

Vincent, C., Mesa, T., & Munné-Bosch, S. (2020). Hormonal interplay in the regulation of fruit ripening and cold acclimation in avocados. *Journal of Plant Physiology, 251*, Article 153225. https://doi.org/10.1016/j.jplph.2020.153225

Webb, M. E., Smith, A. G., & Abell, C. (2004). Biosynthesis of pantothenate. *Natural Product Reports, 21*, 695–721. https://doi.org/10.1039/b316419p

Wysokinska, H., Skrzypek, Z., & Kunert-Radek, J. (1992). Studies on iridoids of tissue cultures of penstemon serrulatus: Isolation and their antiproliferative properties. *Journal of Natural Products, 55*(1), 58–63.

Zhang, Z., Huber, D. J., & Rao, J. (2013). Antioxidant systems of ripening avocado (*Persea americana* Mill.) fruit following treatment at the preclimacteric stage with aqueous 1-methylcyclopropene. *Postharvest Biology and Technology, 76*, 58–64. https://doi.org/10.1016/j.postharvbio.2012.09.003